Classification Techniques Applied in Wood Logs Tomographic Image

Antonio Alberto Pereira Junior
School of Technology
University of Campinas
R. Paschoal Marmo 1888, Limeira/SP, Brazil
ORCID: 0000-0002-2304-3068

Marco Antonio Garcia de Carvalho
School of Technology
University of Campinas
R. Paschoal Marmo 1888, Limeira/SP, Brazil
ORCID: 0000-0002-1941-6036

***Abstract*—The forestry assessment field uses the Non-Destructive Tests (NDTs) to analyze woods logs. To assist the identification of anomalies inside the trunks, the ultrasonic tomography can be used as an alternative. With this technique is possible to evaluate the internal conditions of wooden trunks, through wave propagation applied at specific points. To help the identification and analysis of defects in the tomographic image, this work uses resources from the area of Machine Learning approach in order to identify tomographic images with anomalies. In this study is considered three different classifiers: K-Nearest Neighbors (k-NN), Support Vector Machine (SVM) and Convolutional Neural Network (CNN). The experiments performed were compared using metrics: Accuracy, Precision and Recall. To carry out the experiments, a dataset with 5000 ultrasonic tomography images was build using the Data Augmentation process. In the first experiment, the metrics are calculated based on texture descriptors. The best accuracy results obtained for the CNN, SVM and k-NN models were respectively 89.00%, 80.70% and 79.81%. In the second experiment, the anomaly segmentation was performed with Otsu's segmentation, then it was tested in the SVM classification model. The results found that the SVM model has superior results of demarcation when compared to the CNN model.**

***Index Terms*—Ultrasonic tomography, Non-Destructive Tests, Wood defects**

I. Introduction

There are many factors that contribute to the natural forests reduction, such as: natural phenomena, fires, cutting of trees for commercial purposes and devastation of land for farming activities. In terms of commercial purpose, private landowners who intend to deforest areas for livestock or cutting trees, tend to invest in assertive methods for clearing natural forests, destroying only trees that are of interest and have commercial value. These methods evaluate the internal conditions of the trees before cutting, verifying whether or not the wood is in a good condition before being sold. The trees with low quality do not have high commercial value, but they can be part of the preservation of the forest, as they are important as seed producers, food sources and shelter for animals [1].

The Non Destructive Tests (NDTs) are studied as they allow the internal evaluation of the test specimen while preserving the integrity of the object. The NDTs are interesting for scientists to decide what information is needed to characterize each wood and to know how to use the information to explain the behavior of wood [2]. One of the most known non-destructive techniques applied to trees is the ultrasonic tomography.

This technique allow the evaluation of internal conditions of trunks, by measuring the wave propagation time in the wood logs, without the need to damage the specimen. Therefore, one of the main tasks of ultrasonic tomography is the identification of defects in wood. With regard to the types of wood defects studied, the following can be mentioned: artificial hollows [3], fungal decomposition [4], cracks [5] and termite attack [6]. The images generated by ultrasonic tomography can be improved with spatial interpolation techniques.

The use of computational tools is also required. These tools are capable of generating images that reconstruct the internal properties of the wood. In summary is essential the continuous research for solutions that can handle the generation of images and the identification of defects through ultrasonic tomography in wood logs. The automation to identify the defects in wood is also important, since there would be no need for a specialist to identify the presence or absence of anomalies in the wood.

A. Related works

There are several of works that demonstrate the wide use of the ultrasonic tomography, considering: different types of interpolation methods, experiments setup, organization of transducers, evaluation of the quantitative analysis and improvements of the tomograms.

Primarily, we can cite some works that focus on understand the behavior of ultrasonic tomography in wood, by understanding the relationships about: the coupling of transducers in the wood, problems related to the anisotropy of the wood, signal attenuation, number of measurement points, frequency used in the test, arrangements or meshes for the test and type of transducers ([7], [8], [4], [6]).

The use of spatial interpolation algorithms is also reported in some works, with the goal of reconstructing the internal characteristics. In [9], an approach is presented using affected zones through an ellipse with the same eccentricity. This method was further improved considering ellipses with different eccentricities, giving rise to the Ellipse Based Spatial Interpolation (EBSI) [10]. As a way of evaluating wood considering different axes, the author [11] performs an

experiment with the Radial and Longitudinal axes, and also proposes the method Velocity Correction Interpolation (VCI).

The quantitative analysis to verify the accuracy of the image is also something relevant to research. In [12], it is presented a proposal for quantitative evaluation through the confusion matrix. In [13] and [5] is presented improvements to the interpolation method Ellipse Based Spatial Interpolation (EBSI).

For the identification of defects, some works use artificial intelligence, specifically the artificial neural network [14], [15]. The reconstruction of the internal characteristics of wood using AI is also related in [16], [17]. However, in these works other types of inspection techniques are considered, like: CT and X-ray.

The use of artificial intelligence for identifying defects in wood logs is increasing. Nevertheless, there are opportunities to be developed, precisely because ultrasonic tomography that address the classification and identification of anomalies are not often found, with the exception of the work [5]. In that work, a dataset with 10,000 images is created, to ensure that the samples are sufficient during the training of the classification network. The dataset was generated using software that simulates the internal defects of the wood. The defects were randomly generated according to: location, quantity, shape and transducer number. However, the work does not specifically report how the dataset is generated, only that real and artificial log defects were used. Furthermore, the dataset is not available in a repository, which makes it difficult to validate and reproduce the results. To cover this gap in ultrasonic tomography studies applied to wood, this work intends to implement classification techniques for the identification of defects in different wood species.

B. Objective

This work aims to classify images generated by ultrasonic tomography in wood logs to identify anomalies. To achieve the results, supervised algorithms will be used, specifically: k-Nearest-Neighbor (k-NN) and Support Vector Machine (SVM). As an attempt to compare with the recent works, a Deep Learning approach will also be used through a Convolutional Neural Network (CNN) architecture.

Additionally, this work intends to make a comparison between the classification results by using a confusion matrix, so the metrics Accuracy, Recall and Precision will be used. As a secondary objective, it is proposed to gather data of experiments to generate a dataset.

II. Proposed Approach

This work is organized in the follow main steps: Dataset construction, Data preprocessing, Classification and Analysis of the results. The steps are illustrated in the Figure 1.

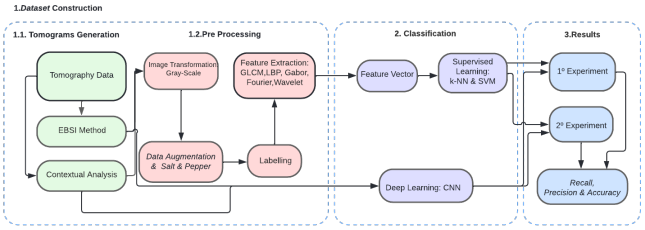

Fig. 1. Proposed Flowchart.

All the steps of the process flow will be discussed in the following subsection.

A. Dataset

The dataset creation is a essential process to further use the tomography images in the classification model. In this work, it will be used the wood logs available from the work [18].

In order to generate the tomograms, these wood logs will be submitted to a test, which consists of measuring the propagation time between the transducers organized by a diffraction mesh.

The choice of the interpolation methods to estimate the unmeasured data will be also required. Two methods will be utilized: The Ellipse Based Spatial Interpolation (EBSI) and the Contextual Analysis. After the interpolation process, a computer program will generate tomography images.

B. Feature Extraction

The extraction of features is a phase that precede the classification. This step is exclusive to the k-Nearest-Neighbor (k-NN) and Support Vector Machine (SVM), as the Convolutional Neural Network (CNN) does not require the feature extraction. In [19] the experiments were performed only with the descriptors Grey Level Coocurrence Matrix (GLCM) and Local Binary Pattern (LBP). In the interest of expand the variety of the results, the following descriptors will be added: Hu Moments, Gabor Filter, Wavelet Transformation, and Fourier Transformation.

C. Classification

The goal of this works is to use machine learning to categorize image that presents anomalies. Due to the reduced amount of machine learning applications in wood logs, this study has an exploratory nature.

In supervised learning, specifically in classification, samples of desired inputs and outputs are presented to the model, which was previously defined by an expert and as a result the model must associate inputs and outputs to all the data. In the case of tomography images, two classes will be considered: defect region and healthy region. These regions will be obtained through Non-destructive testing laboratory (LabEND) assays, which were previously labeled by an expert.

Two classification techniques will be studied: k-Nearest-Neighbor (k-NN) and Support Vector Machine (SVM). These two techniques were chosen because of their common use in classification on CT images. The application of k-NN will be

done in an exploratory way, it is expected to note whether metrics such as: accuracy, recall and precision are improved by a k, in particular, when associated with the descriptors. On the other hand, the SVM will also be applied to tomography images with several parameters, among them, different types of Kernel will be used, such as: Linear, RBF, Polynomial and Sigmoid.

A Deep Learning approach will also be used as an effort to compare the classification performance with the supervised technique. The architecture that will be used is the MobileNets combined with the Single Shot MultiBox Detector (SDD). The MobileNetV2 architecture will be used to produce the *feature maps*, and the fully connected layer will be replaced by the SDD classification network.

The main reason for choosing the SDD-MobileNetV2 architecture is to perform a comparison with the classification results of recent works. In [5] the SDD-MobileNetV2 architecture was used to support and to improve the data interpolation.

D. Comparison

Finally, a comparisons between the classification models is proposed. The confusion matrix is a validation matrix that calculates the classification results. The metrics derived from the matrix are: accuracy, recall e precision.

The accuracy will be used to give an overview of the performance of each model. The *recall* metric will give us an idea of the sensitivity of the model, to predict the proportion of hits for the positives. Finally, the *precision* metric gives us an idea of precision, that is, what is the proportion of correct answers for the classes predicted as positive.

III. Results and Discussion

This section presents the results of the classification models for tomography images and also the quantitative analysis of the metrics obtained by the confusion matrix: accuracy, recall and precision.

A. Dataset creation

The equipment used to measure the time propagation was the *USLab, Agricef*, Brazil with 45kHz frequency and exponential transducers. The test generated the images through a computer program, using interpolation methods. The Figure 2 illustrates the result of the images with the methods on the wood log *Liquidambar styraciflua*.

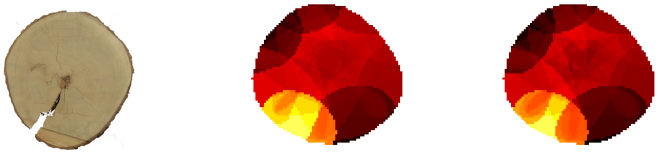

(a) (b) (c)

Fig. 2. Image of the result of the ultrasonic tomography. (a) Image of the wooden log: *Liquidambar styraciflua*. (b) Interpolation by method: *Ellipse Based Spatial Interpolation*. (c) Interpolation by method: Contextual Analysis. Source: [18].

Each wood logs available in LabEND resulted in two different tomograms, the first tomogram was obtained by the Ellipse Based Spatial Interpolation (EBSI) interpolation method and the second by the Contextual Analysis method. Initially 5 logs of different woods were available, at the end, 10 different image tomography were generated.

After generating the images, the Data Augmentation step to increase the amount of available images and the quality of the data [20]. Regarding the approach, this work will use based on geometric transformations and techniques based on color transformations. The Table I details the transformation and parameters used.

Transformation	**Parameters**
Rotation	30°, 60°, 90 °, -30°, -60°e -90 °.
Saturation	Increase of 10% Saturation.
Brightness	Increase of 30% Brightness.
Contrast	Increase of 25% Contrast.
Blur	Addition of 5% blur.
Re dimension	Zoom In of 15% .
Re dimension	Zoom Out of 30% .
Color scale	Transformation to the gray-scale.

TABLE I
TECHNIQUE DESCRIPTION OF DATA AUGMENTATION APPLIED IN THE TOMOGRAPHY IMAGES.

As an attempt to increase even more the dataset, the images were submitted to the addition of Salt & Pepper noise.

B. Feature Extraction

To perform the classification is required a feature extraction for each tomography image. First, the images were transformed into gray-scale and then the characteristics were computed. The Table II shows each of the descriptors and the characteristics used to form the vectors.

Descriptor	**Feature**
Grey Level Coocurrence Matrix (GLCM)	Contrast, Dissimilarity, Homogeneity, Energy, Correlation and Angular second moment (ASM)
Local Binary Pattern	Energy & Entropy
Hu Moments	$H_1, H_2, H_3, H_4, H_5, H_6$ e H_7
Gabor Filter	Energy & Entropy
Wavelet Transformation	Coefficients
Fourier Transformation	Coefficients

TABLE II
DESCRIPTION OF DESCRIPTORS WITH METRICS FOR THE FORMATION OF FEATURE VECTORS.

The assignment of the pixels that indicates the regions with defects and the regions that is healthy is required. Two classes were defined: class (1) for the hollow region, and class (2) for the healthy region of the wood.

The feature vectors generated by the descriptors were further used as an input to the SVM and k-NN classification models. However, it is still necessary to validate the balancing of classes for the classification. As previously mentioned, for all tomography images, the hollow regions and the healthy regions were already known from the previous works available by LabEND. This implies the construction of a biased *dataset*, with all images labeled correctly.

To avoid a possible problem of *bias* in *dataset*, 20% of class assignments were inverted. Images with inverted classes were randomly defined so that there was no intervention in the construction of the classification model.

For the execution of the classification models, the *dataset* was separated into two parts, with 70% of the images for the training phase and 30% of the images for the test phase. The two experiments of this work are explained below.

C. First Experiment

The first experiment refers to the study of different parameters for the classification models of images with a healthy region and images with an anomaly region. The *Kernel*: Linear, *Polynomial*, RBF and *Sigmoid*, was used in the SVM classifier. In the k-NN, different values of k were used. These values were defined through a small experiment with the Local Binary Pattern (LBP) and Gray Level Co-occurrence Matrix (GLCM). Initially the value of k was incremented from k=1 to k=150 for both descriptors. During this attempt, it was noticed that the values of k had more expressive accuracy values for the values k=50, k=100 and k=150. Therefore, it was agreed that the values of k for all descriptors will be: k=50, k=100 and k=150.

As an attempt to evaluate the performance of classified SVM and k-NN, the cross-validation approach will be used.

1) Supervised Learning: First, the different configurations of the SVM model are presented. Table III displays the results of the SVM model with different types of *Kernel*. The top performer for each metric is highlighted in bold.

Model	SVM ($Kernel$) - Descriptor	Accuracy (%)	Recall (%)	Precision (%)
(a)	SVM (Linear) - LBP	78.98	78.42	79.51
(b)	SVM (Linear) - GLCM	79.43	80.23	79.12
(c)	SVM (Linear) - Gabor	63.46	81.97	60.00
(d)	SVM (Linear) - TWD	57.83	51.12	59.35
(e)	SVM (Linear) - TF	74.66	76.30	74.14
(f)	SVM (Linear) - Hu Moments	79.86	78.68	**80.82**
(g)	SVM (Polynomial) - LBP	78.57	76.88	79.77
(h)	SVM (Polynomial) - GLCM	70.02	54.33	79.51
(i)	SVM (Polynomial) - Gabor	62.60	71.22	60.97
(j)	SVM (Polynomial) - TWD	70.66	54.05	80.00
(k)	SVM (Polynomial) - TF	77.33	62.12	78.46
(l)	SVM (Polynomial) - Hu Moments	71.71	58.13	80.18
(m)	SVM (RBF) - LBP	67.87	48.30	79.84
(n)	SVM (RBF) - GLCM	79.15	79.87	78.89
(o)	SVM (RBF) - Gabor	63.57	88.90	59.16
(p)	SVM (RBF) - TWD	80.23	80.74	80.15
(q)	SVM (RBF) - TF	**80.30**	80.60	80.34
(r)	SVM (RBF) - Hu Moments	79.83	79.93	79.96
(s)	SVM (Sigmoid) - LBP	50.28	**99.98**	50.28
(t)	SVM (Sigmoid) - GLCM	67.58	66.63	68.12
(u)	SVM (Sigmoid) - Gabor	49.90	49.70	50.26
(v)	SVM (Sigmoid) - TWD	65.93	57.89	69.28
(w)	SVM (Sigmoid) - TF	65.36	68.82	64.67
(y)	SVM (Sigmoid) - Hu Moments	20.43	20.90	20.87

TABLE III
EFFECTIVENESS OF THE SVM CLASSIFIER USING DIFFERENT COMBINATIONS OF *Kernel* AND DESCRIPTOR. (IN BOLD, THE HIGHEST OBSERVED VALUE OF EACH COLUMN).

The performances shown in Table III show relevant results for SVM models. In order to verify if there are improvements in the SVM model, another experiment is carried out with the combination of the descriptors that obtained the best accuracy results. According to Table III, the descriptors that had consistency in good results were: LBP, GLCM and TWD. The table IV below shows the results of combining these descriptors for the different types of *Kernel*.

Modelo	SVM ($Kernel$) - Descritor	Accuracy (%)	Recall (%)	Precision (%)
(x)	SVM (Linear) - LBP & GCLM	80.16	80.67	80.09
(z)	SVM (Linear) - LBP & TWD	66.00	60.55	68.33
(aa)	SVM (Linear) - GCLM & TWD	60.43	28.39	80.33
(ab)	SVM (Polynomial) - LBP & GCLM	79.56	80.80	79.08
(ac)	SVM (Polynomial) - LBP & TWD	80.43	80.07	80.88
(ad)	SVM (Polynomial) - GCLM & TWD	80.46	80.14	80.89
(ae)	SVM (RBF) - LBP & GCLM	80.26	80.74	80.21
(af)	SVM (RBF) - LBP & TWD	**80.70**	**80.83**	**81.31**
(ag)	SVM (RBF) - GCLM & TWD	80.36	80.60	80.44
(ah)	SVM (Sigmoid) - LBP & GCLM	61.70	62.14	61.93
(ai)	SVM (Sigmoid) - LBP & TWD	80.36	80.41	80.57
(aj)	SVM (Sigmoid) - GCLM & TWD	76.60	70.79	81.04

TABLE IV
PERFORMANCE COMPARISON BETWEEN THE BEST SVM CLASSIFIERS (IN BOLD, THE HIGHEST OBSERVED VALUE OF EACH COLUMN).

According to Tables III and IV, it can be seen that model (y) presents the worst results for all metrics. The models (s) and (o) have high recall values, but low accuracy values.

Likewise, we can highlight the model (l) and (m). These models have considerable accuracy, precision values but low recall values. In this case, the model has a high False Negative (FN) value, so, if there is a defect in the wood, it is not possible to identify with conviction. According to Table IV, improvements can be observed in the results of the metrics, regarding the best model we can highlight (af).

The second phase of the experiment consists of analyzing the k-NN classifier. The Table V shows the results of the k-NN model considering the following values of k: 50, 100 and 150.

In the case of the *k-NN* classifier, the best accuracy results were obtained by the Hu Moments descriptor, with the models: (ap), (av), (ba). Therefore, using the same approach of the SVM , the combination of LBP, GLCM and TWD descriptors will be performed. The Table VI illustrates the results of the combination, considering k: 50, 100 and 150.

The results shown in Tables III and VI show good accuracy values. It can be seen that the results were similar between the descriptors. However, there was no better result when compared to the SVM classifier. According to Table VI it is not possible to identify improvements in the metrics when the descriptors are combined. Finally, the best models considering

Model	k-NN (k) - Descriptor	Accuracy (%)	Recall (%)	Precision (%)
(ak)	k-NN (k=50) - LBP	79.43	80.17	79.19
(al)	k-NN (k=50) - GLCM	79.13	79.85	78.87
(am)	k-NN (k=50) - Gabor	62.70	72.21	60.87
(an)	k-NN (k=50) - TWD	79.60	79.13	79.78
(ao)	k-NN (k=50) - TF	79.50	80.49	78.81
(ap)	k-NN (k=50) - Hu Moments	**79.81**	79.93	**79.93**
(aq)	k-NN (k=100) - LBP	79.45	80.09	79.26
(ar)	k-NN (k=100) - GLCM	79.16	79.93	78.87
(as)	k-NN (k=100) - Gabor	62.94	75.31	60.57
(at)	k-NN (k=100) - TWD	79.55	78.85	79.86
(au)	k-NN (k=100) - TF	79.42	**80.51**	78.68
(av)	k-NN (k=100) - Hu Moments	79.80	79.93	79.91
(aw)	k-NN (k=150) - LBP	79.46	80.11	79.27
(ay)	k-NN (k=150) - GLCM	79.10	79.95	78.77
(ax)	k-NN (k=150) - Gabor	62.98	76.17	60.46
(ay)	k-NN (k=150) - TWD	79.43	78.51	79.88
(az)	k-NN (k=150) - TF	79.37	80.49	78.61
(ba)	k-NN (k=150) - Hu Moments	79.80	79.93	79.90

TABLE V
EFFECTIVENESS OF THE k-NN CLASSIFIER USING DIFFERENT COMBINATIONS OF *Kernel* AND DESCRIPTOR. (IN BOLD, THE HIGHEST OBSERVED VALUE OF EACH COLUMN).

Model	SVM ($Kernel$) - Descritor	Accuracy (%)	Recall (%)	Precision (%)
(bb)	k-NN (k=50) - LBP & GLCM	79.13	**79.95**	78.85
(bc)	k-NN (k=50) - LBP & TWD	63.26	36.20	79.85
(bd)	k-NN (k=50) - GLCM & TWD	62.86	35.98	80.70
(be)	k-NN (k=100) - LBP & GLCM	**79.17**	79.95	78.91
(bf)	k-NN (k=100) - LBP & TWD	61.40	31.23	79.86
(bg)	k-NN (k=100) - GLCM & TWD	60.70	30.57	80.44
(bh)	k-NN (k=150) - LBP & GLCM	79.14	79.95	78.86
(bi)	k-NN (k=150) - LBP & TWD	60.43	28.39	80.33
(bj)	k-NN (k=150) - GLCM & TWD	59.80	27.83	**81.17**

TABLE VI
PERFORMANCE COMPARISON BETWEEN THE BEST SVM CLASSIFIERS (IN BOLD, THE HIGHEST OBSERVED VALUE OF EACH COLUMN).

the accuracy of the k-NN classifiers are the models that consider the Hu Moments descriptor.

2) Deep Learning: The last classification method discussed in this work was the CNN. In this case, the experiment consists of comparing one of the best performances of SVM and k-NN, with the results obtained using SDDMobileNetV2 architecture. The Table VII shows the results.

Model	Description	Accuracy (%)	Recall (%)	Precision (%)
(bk)	SDDMobileNetV2	**89.00**	**93.40**	**97.30**
(ap)	k-NN (k=50) - Hu Moments	79.81	79.93	79.93
(af)	SVM (RBF) - LBP & TWD	80.70	80.83	81.31

TABLE VII
PERFORMANCE COMPARISON (IN BOLD, THE HIGHEST OBSERVED VALUE OF EACH COLUMN).

In Table VII, the performance of the SDDMobileNetV2 classifier was in all cases superior to the performance obtained by the other classifiers. However, these results refer to the task of classifying the tomography image that contains or does not contain the anomaly. The results shown above do not show the specific region of the image associated with the anomaly.

D. Second Experiment

The second experiment intends to specifically identify and classify the region of the anomaly in the tomograms. For this, the images were submitted to the Otsu [21] segmentation. The use of Otsu technique is unique to the SVM and k-NN models, as CNN uses the bounding box approach to perform region classification. First, all tomography images from the *dataset* were submitted to the Otsu segmentation. After the segmentation process, two images are generated, the first referring to the healthy region and the other referring to the defect region. Afterwards, the trained classification model will identify which class the images belong to.

The Figure 3 illustrates the results of different wood types for defect region classification. In the following images, the supervised model that obtained the best performance in the previous experiment and the CNN model are used as a comparison. Thus, the first column of images ((a),(d),(g),(j),(m)) illustrates the images of wood, the second column ((b),(e),(h) ,(k),(n)) uses the SVM classifier (RBF) - LBP & TWD and the third column of images ((c),(f),(i),(l),(o)) uses the SDDMobileNetV2 network model.

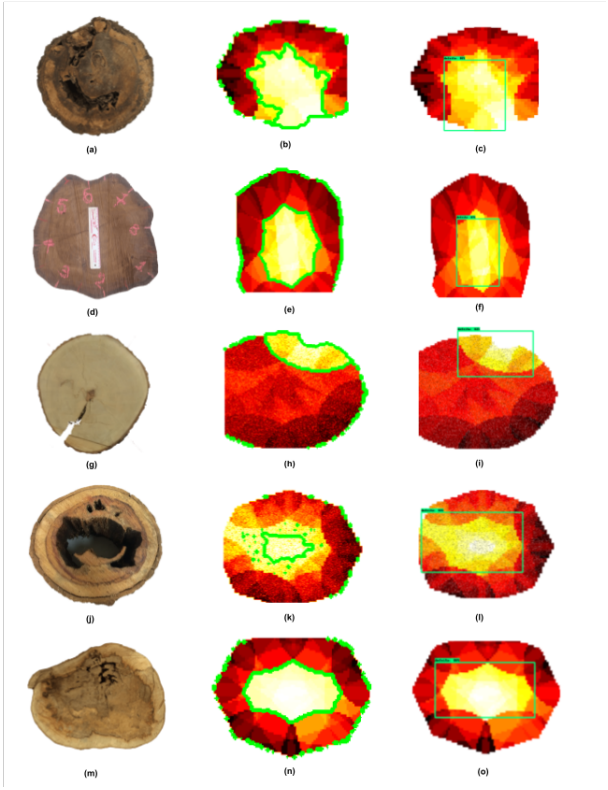

Fig. 3. Region ranking comparison between models: SVM (RBF) - LBP & TWD and SDDMobilenetV2. First column: wood logs; Second column (SVM); Third column (CNN).

Regarding the images with the supervised model, observe the presence of defects in the regions delimited by Otsu

technique (region in green). Compared to the CNN model, this information is more accurate when compare to the original wood image. This defect detection is relevant from the point of view of classifying the use of wood, specially for commercial purposes.

IV. Discussion

This work presents a comparative study of classification through two experiments. The first experiment refers to the classification of tomography images with anomaly or defects. For this, the experiment uses supervised methods: *k*-NN, SVM, CNN and different types of texture descriptors. The second experiment compares the classification of the region. In this second experiment, the supervised SVM method is compared with Otsu's segmentation, and the Network SDDMobileNetV2, which uses the object detection approach for classification. In the result of the first experiment, it was possible to identify the classification techniques and the descriptors that helped for the best results of *accuracy, recall* and precision. Therefore, it is essential to choose the descriptors with the combination of classification algorithms for the composition of results in tomography images.

The result of the second experiment concerns the classification of the location of the anomaly in the tomography image. As mentioned, in the work of [5], a reconstruction of tomography images using a *Convolutional Neural Network* (CNN) was proposed. This technique was used to detect the size, texture and limit the outline of defects in the wood. In this work, a dataset consisting of 5,000 tomography images is used. Despite this, the data set created by the authors is not available, making it impractical to compare it with other anomaly identification approaches. Due to the difficulty of comparison, in this work, there was a need to generate a set of data with the addition of data augmentation techniques for the implementation of CNN. After generating the data set, this work makes a comparison between: a CNN with the object detection approach and an anomaly identification model through the segmentation process with the Otsu method.

The results obtained by this work have *accuray, recall* and precision results greater than 89%. In [5]'s work, the *Stress Wave* technique is used as Non-Destructive Testing (NDT) and the EBSI interpolation method for image generation. At work, improvements are also made to the SDD MobileNet network to delimit the defect region. Although the accuracy of the classification models of this work are not superior to that of [5], whose accuracy is 93.6%, this work proposes a comparative study of classification techniques for the identification of anomaly, with images of different species of wood obtained by ultrasonic tomography and interpolation methods.

V. Conclusion

Acoustic methods have been used as an alternative to Non-Destructive Testing (NDTs) in the forest area, especially the ultrasonic tomography method, as it is cheap and portable. Images of the inside of wooden logs shows the internal structures and features, which can be reconstructed by using interpolation algorithms.

In this work, a study on the use of data classification techniques in wood tomography images is presented. Our dataset is composed of images obtained in tomography, a non-destructive method capable of evaluating the internal characteristics of wood logs without causing damage.

In order to identify whether an image has anomalies or not, three different image classification methods were applied: k-NN, SVM and CNN with SDDMobilenetV2 architecture. The performance of these methods was evaluated according to the *accuracy, precision* and recall metrics, calculated from a confusion matrix constructed based on the classification results. We also performed a classification task of the image region, in order to obtain the region corresponding to the wood anomaly.

Our first experiments showed that the best results are obtained by the convolutional classifier, specifically for the metrics accuracy and precision. For this classifier, the values of *accuracy, precision* and recall are greater than 85%. A last experiment carried out in this work was dedicated to identifying the region in the image associated with the internal defect. In this case, the defect identification by the Otsu method obtained a more detailed result on the shape and size of the defect when compared to the convolutional classifier, which displays the defect in a rectangular format. Due to the difficulties in obtaining tomography images, our contribution is also associated with the creation of a *dataset* composed of 5000 images using the Data Augmentation technique.

There are several suggestions for future work. First, to improve the variability of the dataset, we need more tomographic images of wood from different species and types of anomalies. Furthermore, the use of a combination of texture descriptors of different types should be the subject of future studies. There is also a suggestion to use a classifier with the image segmentation approach, instead of an object detection approach. And finally, as future work, we would like to properly identify the anomaly, its location and dimensions.

VI. Acknowledgment

This study was financed in part by the Coordenação de Aperfeiçoamento de Pessoal de Nível Superior – Brasil (CAPES) – Finance Code 001.

References

[1] P. Amaral, A. Veríssimo, P. Barreto, and E. Vidal, "Floresta para sempre: um manual para a produção de madeira na amazônia," WWF, Brasilia, DF (Brasil) Instituto do Homem e Meio Ambiente da Amazonia, Tech. Rep., 1998.

[2] V. Bucur, *Acoustics of wood*. Springer Science & Business Media, 2006.

[3] S. Brazolin, "Biodeterioração, anatomia do lenho e análise de risco de queda de árvores de tipuana, tipuana tipu (benth.) o. kuntze, nos passeios públicos da cidade de são paulo, sp," 2009.

[4] C. J. Lin, Y. C. Kao, T. T. Lin, M. J. Tsai, S. Y. Wang, L. D. Lin, Y. N. Wang, and M. H. Chan, "Application of an ultrasonic tomographic technique for detecting defects in standing trees," *International Biodeterioration and Biodegradation*, vol. 62, no. 4, pp. 434–441, 2008.

[5] X. Du, J. Li, H. Feng, and H. Hu, "Stress wave tomography of wood internal defects based on deep learning and contour constraint under sparse sampling," in *Intelligence Science and Big Data Engineering. Big Data and Machine Learning*, Z. Cui, J. Pan, S. Zhang, L. Xiao, and J. Yang, Eds. Cham: Springer International Publishing, 2019, pp. 335–346.

[6] S. Palma, R. Goncalves, A. Trinca, C. Costa, M. Reis, and G. Martins, "Interference from knots, wave propagation direction, and effect of juvenile and reaction wood on velocities in ultrasound tomography," *BioResources*, vol. 13, no. 2, pp. 2834–2845, 2018.

[7] L. V. Socco, L. Sambuelli, R. Martinis, E. Comino, and G. Nicolotti, "Feasibility of ultrasonic tomography for nondestructive testing of decay on living trees," *RESEARCH IN NONDESTRUCTIVE EVALUATION*, vol. 15, pp. 31–54, 01 2004.

[8] V. Bucur, "Ultrasonic techniques for nondestructive testing of standing trees," *Ultrasonics*, vol. 43, no. 4, pp. 237 – 239, 2005. [Online]. Available: http://www.sciencedirect.com/science/article/pii/S0041624X04002367

[9] L. Zeng, J. Lin, J. Hua, and W. Shi, "Interference resisting design for guided wave tomography," *Smart Materials and Structures*, vol. 22, no. 5, p. 055017, 2013. [Online]. Available: https://doi.org/10.1088%2F0964-1726%2F22%2F5%2F055017

[10] X. Du, S. Li, G. Li, H. Feng, and S. Chen, "Stress wave tomography of wood internal defects using ellipse-based spatial interpolation and velocity compensation," *BioResources*, vol. 10, no. 3, pp. 3948–3962, 2015.

[11] H. Feng, Z. Qian, M. Hu, Z. Zheng, and X. Du, "The study of stress wave tomography algorithm for internal defects in rl plane of wood," in *2018 Chinese Automation Congress (CAC)*, 2018, pp. 2283–2288.

[12] J. Strobel, M. Carvalho, R. Gonçalves, C. Pedroso, M. Reis, and P. Martins, "Quantitative image analysis of acoustic tomography in woods," *European Journal of Wood and Wood Products*, vol. 76, 06 2018.

[13] X. Du, J. Li, H. Feng, and S. Chen, "Image reconstruction of internal defects in wood based on segmented propagation rays of stress waves," *Applied Sciences*, vol. 8, p. 1778, 09 2018.

[14] X.-d. Zhu, J. Cao, F.-H. Wang, J.-p. Sun, and Y. Liu, "Wood nondestructive test based on artificial neural network," in *2009 International Conference on Computational Intelligence and Software Engineering*. IEEE, 2009, pp. 1–4.

[15] H. Mu, M. Zhang, D. Qi, S. Guan, and H. Ni, "Wood defects recognition based on fuzzy bp neural network," *Int. J. Smart Home*, vol. 9, pp. 143–152, 2015.

[16] M. R. Effendi, R. Willyantho, and A. Munir, "Back propagation technique for image reconstruction of microwave tomography," in *Proceedings of the 2019 9th International Conference on Biomedical Engineering and Technology*, 2019, pp. 186–189.

[17] M. Hansson, A. Enescu, and S. S. Brandt, "Knot detection in x-ray images of wood planks using dictionary learning," in *2015 14th IAPR International Conference on Machine Vision Applications (MVA)*. IEEE, 2015, pp. 497–500.

[18] J. R. A. Strobel *et al.*, "Método de interpolação baseado em elipses associado à análise contextual de rotas para geração de tomografias ultrassônicas em toras de madeira," 2017.

[19] A. A. P. Junior and M. A. G. de Carvalho, "An initial study in wood tomographic image classification using the svm and cnn techniques." in *VISIGRAPP (4: VISAPP)*, 2022, pp. 575–581.

[20] C. Shorten and T. M. Khoshgoftaar, "A survey on image data augmentation for deep learning," *Journal of Big Data*, vol. 6, no. 1, pp. 1–48, 2019.

[21] N. Otsu, "A threshold selection method from gray-level histograms," *IEEE transactions on systems, man, and cybernetics*, vol. 9, no. 1, pp. 62–66, 1979.